How clay mineral assemblages affect instability on the upper slope of the Hikurangi subduction zone, New Zealand

Michael B. Underwood [1], Brandon Dugan [2], and Sebastian Cardona [3]

[1] Department of Earth and Environmental Science, New Mexico Institute of Mining and Technology, Socorro, NM USA

[2] Department of Geophysics and Hydrologic Science and Engineering Program, Colorado School of Mines, Golden, CO USA

[3] Department of Geology and Geophysics, Texas A & M University, College Station, TX USA

Corresponding author: Michael Underwood (UnderwoodM@missouri.edu)

Key Points:

- Hikurangi trench-slope sediments, including muds within the Tuaheni landslide complex, contain high concentrations of detrital smectite
- Smectite is abundant enough to reduce the bulk sediment's coefficient of friction, with little stratigraphic variability
- The homogeneous mud composition results from strong currents and does not change significantly along inferred slip surfaces or weak layers

Abstract

The International Ocean Discovery Program cored Sites U1517 (Tuaheni landslide complex) and U1519 (upper Tuaheni Basin) on the Hikurangi margin, North Island, New Zealand. Strong ocean currents result in unusual amounts of compositional homogeny in the muds. Detrital smectite dominates among clay minerals, with average proportions of 52 wt% at Site U1517 and 53 wt% at Site U1519. Bulk sediment from Site U1517 contains up to ~29 wt% smectite (average = 21 wt%), high enough to reduce the angle of internal friction (on average) to ~6°. There are no compositional excursions along inferred slip surfaces or weak layers. Smectite decreases toward the SW in the "downstream" direction of the East Cape Current, and that spatial trend correlates with lower densities of slide scars.

Plain Language Summary

Expandable clay minerals of the smectite group are notorious for weakening soils and marine sediments and contributing to conditions that promote landslides. The Hikurangi margin offshore North Island, New Zealand, is noted for its abundance of submarine landslides. To assess their possible causes, we analyzed clay mineral assemblages from two sites on the upper trench slope that were sampled by the International Ocean Discovery Program (Sites U1517 and U1519). Cores from both sites display unusual degrees of compositional homogeny, with smectite as the dominant clay mineral. Illite occurs in lesser amounts, and the concentrations of chlorite and kaolinite are relatively minor. Cores from Site U1517 encompass the Tuaheni landslide complex, but we did not find any compositional anomalies at inferred slip surfaces or along weak layers. Instead, the entire stratigraphic succession appears to be relatively weak. Because of that inherited preconditioning, dynamic loading during such events as large earthquakes is probably enough to trigger numerous submarine landslides. However, there appears to be no predisposition for slip along any unusually weak, layer-specific interval of the sediment.

1 Introduction

Sedimentary facies in active subduction zones with high rates of terrigenous sedimentation (e.g., Cascadia, Nankai Trough, southern Chile Trench, Sumatra, Makran) are governed by interactions among eustacy, tectonics, and sediment-transport processes (e.g., Piper et al., 1973; Underwood & Bachman, 1982; Thornburg & Kulm, 1987). Subduction accretion normally creates a stair-step series of intraslope basins separated by fault-cored anticlinal ridges (e.g., Moore & Karig, 1976; McAdoo et al., 2004; Ding et al., 2010; Contardo et al., 2011). Some unconfined flows are capable of overtopping bathymetric highs (Muck & Underwood, 1990), but taller ridges tend to block such pathways. Consequently, slope basins behind taller tectonic ridges typically act as traps for turbidity currents, slumps, mudflows, and debris-flows (e.g., Moore & Karig, 1976; Underwood & Moore, 1995; Contardo et al., 2008; Nelson et al., 2011), whereas steeper slopes are usually covered by mud that settles slowly from suspension.

Submarine slides are common in subduction zones (e.g., Yamada et al., 2010; Harders et al., 2011; Hill et al., 2020), but their spatial distributions are challenging to understand, and their triggering mechanisms are often impossible to pin-point. Geotechnical tests provide clues by revealing how frictional properties change with concentrations of individual minerals (e.g., Lupini et al., 1981; Shimamoto & Logan, 1981; Logan & Rauenzahn, 1987; Tiwari & Marui, 2005; Tembe et al., 2010; Ikari et al., 2018). Many additional variables need to be considered, however: seafloor topography; rates of sediment accumulation; grain size distribution, especially the proportion of clay-sized grains; particle shape and microfabric; hydration state of clay minerals; porosity, permeability, and pore-fluid pressure; consolidation and lithification; and dynamic loading by earthquakes (e.g., Hampton et al., 1996; Locat & Lee, 2002; Masson et al., 2006; Bartetzko & Kopf, 2007; Ikari et al., 2007, 2011; Kock & Huhn, 2007; Saffer & Tobin, 2011; Takahashi et al., 2014; Trutner et al., 2015; Kremer et al., 2017; Silver & Dugan, 2020). Those variables seemingly combine in ways that are unique to each individual locale (Vanneste et al., 2014).

The Hikurangi margin offshore North Island, New Zealand (Fig. 1a) conforms to most of the paradigms of subduction-zone tectonics and sedimentation (Bostock et al., 2018). The margin's architecture includes forearc basins, imbricate thrusts and folds within the frontal accretionary prism, and scattered slope basins (e.g., Tuaheni Basin) (Barnes et al., 2002; Paquet et al., 2009; Pedley et al., 2010; Pouderoux et al., 2012; Ghisetti et al., 2016). The landward trench slope is also noteworthy for submarine landslides, including the Tuaheni landslide complex (Collot et al., 2001; Mountjoy et al., 2014b; Watson et al., 2020). Hikurangi deviates from the global paradigm, however, in two important ways: ocean currents are strong, and contourite drifts and hybrid contourites are widespread (Bailey et al., 2020, 2021; Couvin et al., 2020). Mindful of those facts, we focus attention in this paper on how slope-parallel currents affect mud composition across the mid to upper slope. We test whether that composition has had any demonstrable influence on slope stability and landslides. Our results for Hikurangi provide a tightly constrained case study that serves as a benchmark for comparisons of cause-and-effect for slope failures and mass-transport deposits along other margins.

Dispersal and deposition of fine-grained suspended sediment in the oceans are governed by several processes (e.g., Gorsline, 1984; McCave, 1984). Sediment gravity flow provides one mechanism for directing mud onto the Hikurangi slope, as unconfined turbidity currents and/or by funneling through submarine canyons (Mountjoy et al., 2009a, 2014a; Alexander et al., 2010; Pouderoux et al., 2012). Margin-parallel ocean currents provide the main competition (Carter & Wilkin, 1999; Chiswell et al., 2015). The NE-directed Wairarapa Coastal Current (Fig. 1a) carries suspensions along the continental shelf and uppermost slope (Foster & Carter, 1997; Chiswell, 2000). A strong SW-directed current (East Cape Current) dominates the mid to upper slope (Fig. 1a), extending to a water depth of ~1300 m (Chiswell & Roemmich, 1998). Transient counterclockwise gyres (e.g., Wairarapa Eddy) impact surface-water farther offshore (Fig. 1a), but their temporal stability

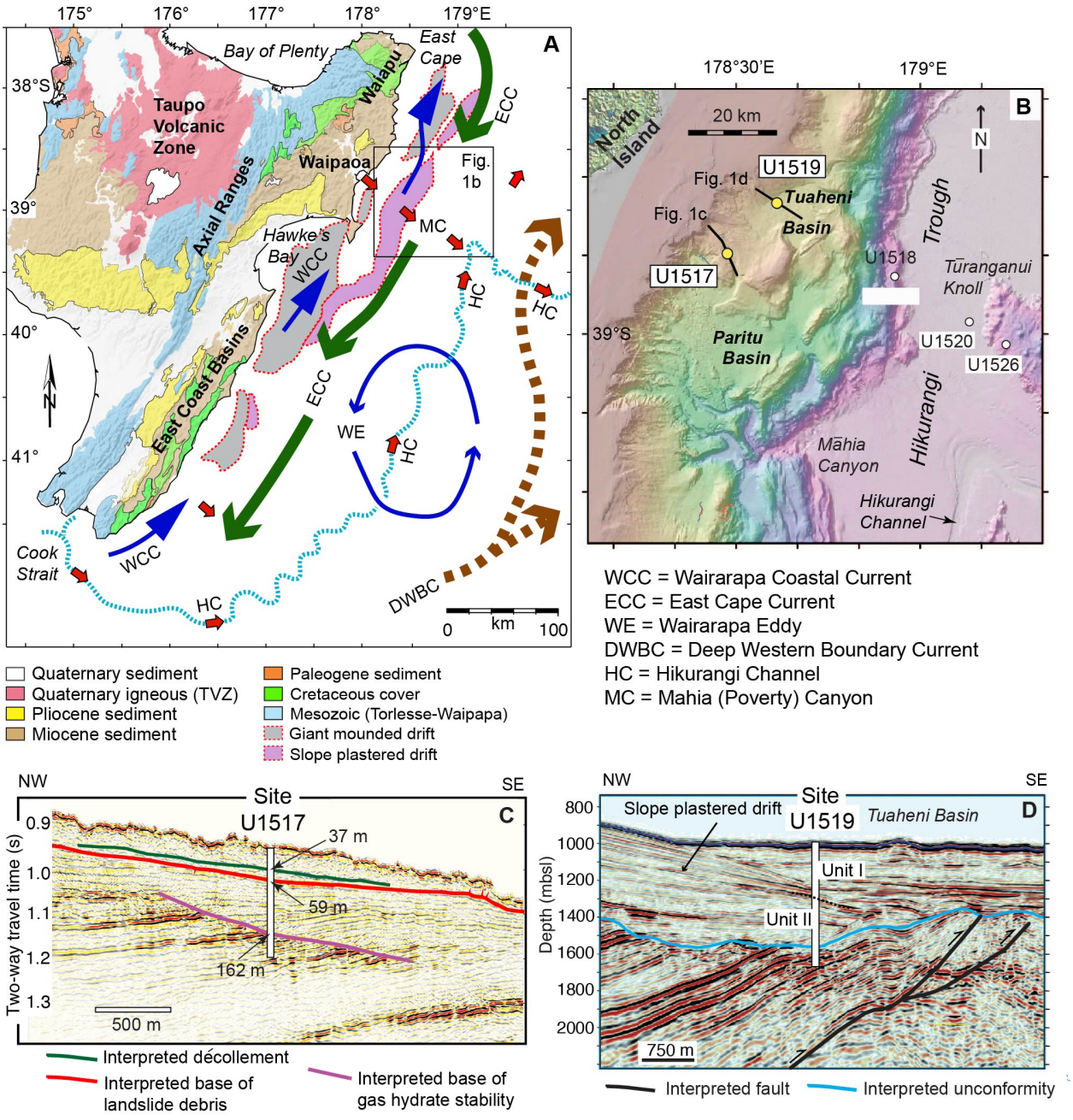

Figure 1. a. Simplified map of onshore geology, North Island, New Zealand (modified from Jiao et al., 2014), prominent bathymetric features, ocean currents, and pathways for sediment transport by gravity flow. Giant mounded drifts and slope plastered drifts from Bailey et al. (2020). b. Bathymetric map with locations of Tuaheni Basin and IODP sites (from Saffer et al., 2017). c. Seismic reflection profile crossing IODP Site U1517. Interpretations from Barnes et al. (2019a). d. Seismic reflection profile crossing IODP Site U1519. Interpretation of slope plastered drift from Bailey et al. (2020). Interpretations of faults and unconformity from Barnes et al. (2019b). See Fig. 1b for tracklines.

and maximum water depths remain uncertain (Chiswell & Roemmich, 1998; Chiswell, 2005). Seaward of the trench, the Deep Western Boundary Current (Fig. 1a) dominates abyssal circulation and drift sedimentation (Carter & McCave, 1997, 2002; Carter et al., 2004). Those currents set up a likelihood of persistent mixing of suspensions from downslope versus along-slope routing.

The International Ocean Discovery Program (IODP) positioned Site U1519 in Tuaheni Basin on the upper trench slope (Fig. 1b), approximately 38 km from shore at a water depth of 1000 m. The site lies well within the domain of the East Cape Current (Fig. 1a), and Bailey et al. (2020, 2021) recognized the nearby acoustic character as a "slope plastered" contourite drift (Fig. 1c). Shipboard sedimentologists (Barnes et al., 2019b) defined two lithostratigraphic units (Fig. 2b). Unit I (0–282.66 mbsf) is composed of mud and mudstone with sparse and very thin interbeds of silt and volcanic ash (Fig. 2b), whereas unit II (282.66–635.65 mbsf) consists of mudstone with scattered interbeds of siltstone, sandy siltstone, and sandstone (inferred turbidites). Some intervals display convolute laminae, mesoscale folds, dismembered bedding, and clasts of mudstone in a mudstone matrix, all suggestive of mass transport. Evidence from cores for contourite deposition is inconclusive. In general, diagnostic criteria remain elusive for distinguishing among turbidites, contourites, hemipelagites, and hybrids (Stow et al., 2002; Stow & Smillie, 2020). Definitive bed-by-bed identification requires time-consuming post-cruise analyses of microstructures, ichnofacies, grain size distributions, mineralogy, geochemistry, and/or computed tomography (e.g., Alonso et al., 2016; Nishida, 2016; Rodriquez-Tovar & Hernandez-Molina, 2018; Vandorpe et al., 2019; de Castro et al., 2020). Unfortunately, rigorous analyses of the cores from Site U1519 were thwarted by wide gaps between intervals of core (Fig. 3b), unusually poor recovery (~55%), and widespread (severe) drilling disturbance. Thus, the prevalence of contourites near Site U1519 is based largely on seismic-reflection interpretations (Bailey et al., 2020).

At a water depth of ~732 m (Fig. 1b), Site U1517 is also well within the core of the East Cape Current (Chiswell et al., 2015), and seismic-reflection data are indicative of a "slope plastered" contourite drift (Bailey et al., 2020, 2021). The primary purpose of drilling Site U1517, however, was to log and sample through the Tuaheni landslide complex (Mountjoy et al., 2014b). Creep seems to have occurred where the base of gas-hydrate stability pinches out at the seafloor (Mountjoy et al., 2009b, 2014b), so one hypothesis is that occlusion of permeability by gas hydrate may have led to overpressured conditions and hydrofracturing (Crutchley et al., 2010; Ellis et al., 2010; Gross et al., 2018). Hydrate-bearing sediments, moreover, might be prone to time-dependent plastic deformation (Mountjoy et al., 2014b). To test those ideas, the cored interval at Site U1517 (Fig. 1d) crossed interpreted positions of the décollement at ~37 mbsf, the base of landslide debris at ~59 mbsf, and the base of gas-hydrate stability at ~162 mbsf (Barnes et al., 2019a).

According to shipboard scientists (Barnes et al., 2019a), unit I at Site U1517 (0–3.0 mbsf) consists of a thin Holocene mud blanket (Fig. 2a). Unit II (3.0–40.74 mbsf) contains interbeds of mud and very fine sand. The

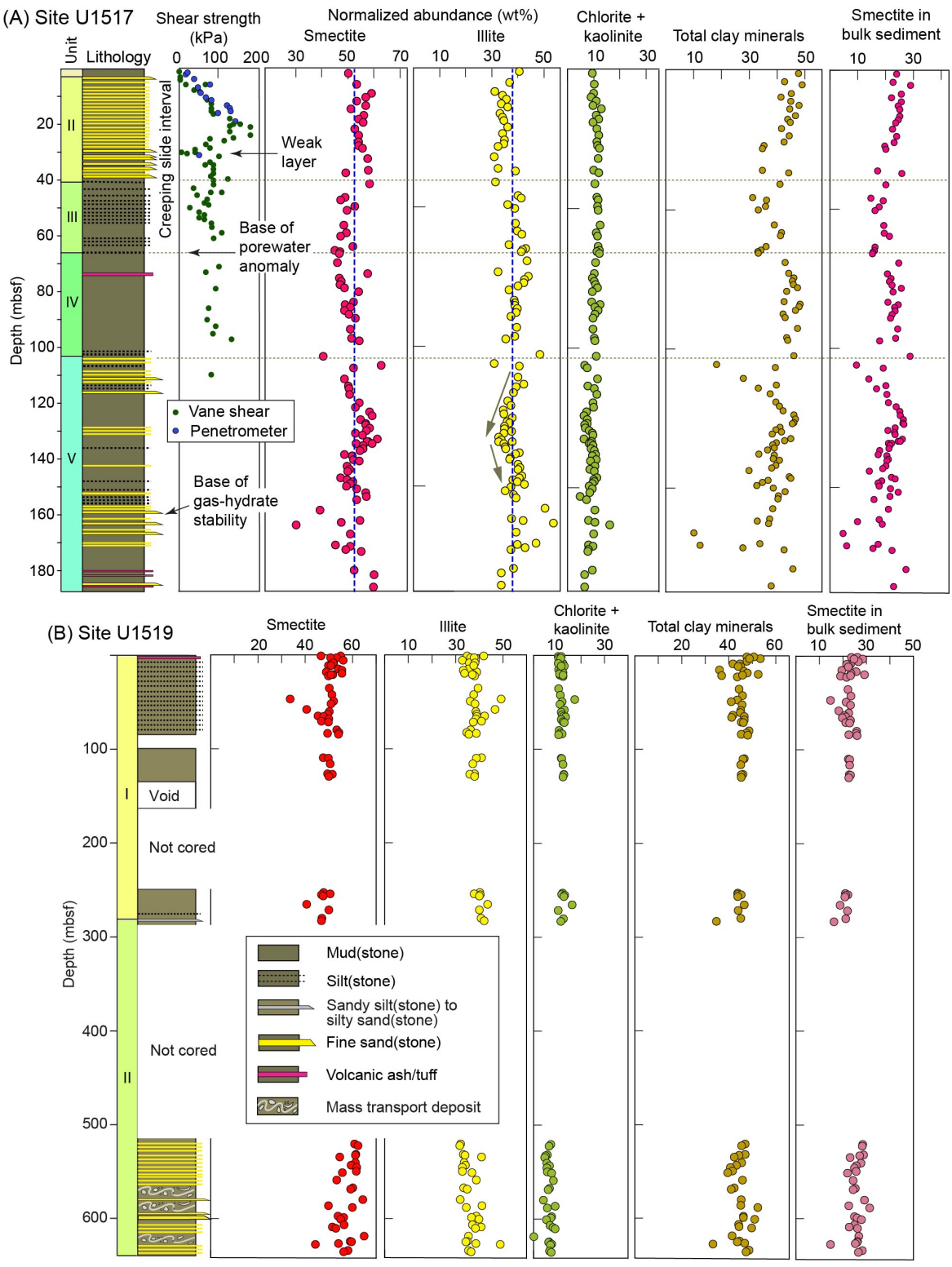

Figure 2. a. XRD results for IODP Site U1517 (Underwood and Dugan, 2021). Proportions of total clay minerals and values of shear strength from Barnes et al. (2019a). b. XRD results for IODP Site U1519 (Underwood 2022). Proportions of total clay minerals from Barnes et al. (2019b).

bioturbated mud within unit III (40.74–66.38 mbsf) alternates with laminated stacked couplets of silt and clay, resembling silty contourites described elsewhere (e.g., Stow et al., 2002; Stow & Smillie, 2020). Unit IV (66.38–103.16 mbsf) consists mostly of structureless mud, whereas unit V (103.16–187.53 mbsf) contains numerous interbeds of normally graded sand (inferred turbidites) and mud (Fig. 2a). Barnes et al. (2019a) provisionally assigned the upper ~67 m of strata to the Tuaheni landslide complex (Fig. 2a), but many questions about the landslide remain. Gas hydrate was detected, for example, but only at depths deeper than 100 mbsf (Barnes et al., 2019a); that observation and numerical modeling indicate that gas-hydrate dynamics are unlikely as the main destabilizing variable (Screaton et al., 2019). Couvin et al. (2020) identified two chaotic acoustic intervals in nearby seismic-reflection profiles, but the correlative intervals of core (units II and III) are perplexing because they display almost no internal deformation; moreover, there are no mesoscopic indicators of concentrated slip at the base of the inferred landslide (Barnes et al., 2019a). The only core-scale indicators of gravity-driven, soft-sediment deformation are scattered patches that display convolute bedding and/or intraformational mud clasts (Barnes et al., 2019a). Couvin et al. (2020) suggested that Hole U1517C intersected an intact block within an otherwise chaotic landslide. Adding to the debate, Luo et al. (2020) used numerical modeling of porewater-chemistry data to support their contention of two slip events. The more-recent failure evidently occurred as a coherent 40-m-thick block, which places the décollement at the base of unit II. On the other hand, shipboard measurements of shear strength (Barnes et al., 2019a) revealed a weak interval centered at ~31 mbsf, within the middle of unit II (Fig. 2a). These conflicting results and interpretations deserve more scrutiny. Our objective here is to determine if excursions in clay mineralogy might be large enough to have affected the sediment's shear strength along any slip surfaces or weak intervals.

2 Materials and Methods

Samples from Sites U1517 and U1519 were positioned with several collocated subsamples ("clusters") adjacent to whole rounds that had already been extracted from cores for tests of interstitial water chemistry and geotechnical/frictional/hydrogeologic properties. Coarser interbeds were avoided. See Underwood and Dugan (2021) for detailed descriptions of sample preparation and XRD methods. To reiterate briefly, mud specimens were disaggregated, and oriented aggregates of glycol-saturated clay-sized splits (<2 μm equivalent spherical settling diameter) were prepared using the filter-peel method (Moore & Reynolds, 1989). XRD scans were completed using a Panalytical X'Pert Pro diffractometer, and values of normalized relative mineral abundance were computed using a set of regression equations that relate wt% values to peak area. Absolute errors of accuracy are: illite = 3.0 wt%, smectite = 3.9 wt%, and undifferentiated (chlorite + kaolinite) = 5.1 wt% (Underwood et al., 2020). Compositional differences among individual specimens, or between lithologic units, are not regarded as geologically significant unless they exceed those errors.

3 Data

The cored intervals at Site U1519 display unusually small amounts of compositional scatter, with minor (but statistically significant) differences between the two lithologic units (Fig. 3b). Results of 76 measurements (Underwood, 2021) show smectite to be the most abundant clay mineral (site average = 53 wt%), with normalized abundances ranging from 33 to 65 wt%. Proportions of illite range from 32 to 49 wt%, and the values for undifferentiated (chlorite + kaolinite) are 0–16 wt%. The mean (μ) and standard deviation (σ) values for unit I are smectite: μ = 50 wt%, σ = 4; illite: μ = 38 wt%, σ = 3; and undifferentiated (chlorite + kaolinite): μ = 12 wt%, σ = 1. Comparable statistics for unit II are smectite: μ = 57 wt%, σ = 5; illite: μ = 36 wt%, σ = 4; undifferentiated (chlorite + kaolinite): μ = 7 wt%, σ = 2.

The ninety-nine specimens from Site U1517 (Underwood & Dugan, 2021) likewise reveal small variations among the five lithologic units (Fig. 2a). Smectite is the most abundant clay mineral (site average = 52 wt%), with a range of 30–63 wt% (Fig. 2a). Percentages of illite range from 31 to 54 wt%, and the range for undifferentiated (chlorite + kaolinite) is 5–16 wt%. The mean and standard deviation statistics for unit II are smectite: μ = 55 wt%, σ = 3; illite: μ = 34 wt%, σ = 2; undifferentiated (chlorite + kaolinite): μ = 11 wt%, σ = 1. Values for unit III are smectite: μ = 48 wt%, σ = 2; illite: μ = 40 wt%, σ = 2; chlorite + kaolinite: μ = 11 wt%, σ = 0.5. Statistics for unit IV are smectite: μ = 51 wt%, σ = 5; illite: μ = 39 wt%, σ = 4; undifferentiated (chlorite + kaolinite): μ = 10 wt%, σ = 1. In unit V, the statistics are smectite: μ = 53 wt%, σ = 5; illite: μ = 38 wt%, σ = 4; undifferentiated (chlorite + kaolinite): μ = 9 wt%, σ = 2. Unit V displays the greatest amount of statistical scatter, with subtle gradients of decreasing, then increasing proportions of illite moving down-section (Fig. 2a). Compositional shifts at horizons of interest (e.g., ~31, ~41, ~66 mbsf) are trivial, however, and within the normal error range for the method (Fig. 2a).

Concentrations of individual minerals in bulk sediment are more diagnostic if the goal is to assess how composition affects hydrogeological, frictional, and geotechnical properties. The average content of total clay minerals at Site U1517 is 40 wt%, with a range of 10–49 wt% (Barnes et al., 2019a). Average values for bulk sediment are: smectite = 1 wt% (σ = 4); illite = 15 wt% (σ = 3); and undifferentiated (chlorite + kaolinite) = 4 wt% (σ = 0.9). Contrasts across unit boundaries are within the background range of scatter, and excursions are absent at the suspected slip surfaces (Fig. 2a). Data from Site U1519 are similar (Fig. 2b).

To expand spatial coverage, we also collected data from 30 specimens from piston and gravity cores (Underwood, 2020), from the vicinity of the Ruatoria debris avalanche in the NE to offshore Hawke's Bay in the SW (Fig. 3a). Smectite ranges from 29 to 54 wt% (μ = 45, wt% σ = 6). The range for illite is 36–57 wt% (μ = 43 wt%, σ = 5), and undifferentiated (chlorite + kaolinite) ranges from 9 to 16 wt% (μ = 12 wt%, σ = 2). These values overlap data from Sites U1517 and U1519, but with more statistical scatter. Moreover, samples

from the NE corner of the study area generally contain more smectite (and less illite) compared to those to the SW (Fig. 3a).

4 Results

4.1. Principal Sources for Detrital Clays

If our results are viewed in the context of geotechnical inquiry, it doesn't really matter where the clays originated, or how they arrived at sites of deposition, but we offer some possibilities. Illite is the expected weathering product of plutonic, low-grade metasedimentary, and sedimentary sources (Biscaye, 1965; Fagel, 2007). Basement rocks across New Zealand (Fig. 1a) consist mostly of illite- and chlorite-rich metagraywackes and argillites of the Torlesse and Waipapa terranes (Sporli, 1978; MacKinnon, 1983; Warr & Cox, 2016). Younger cover sequences and forearc deposits in the East Coast Basin, and in regions immediately southeast of the Axial Range (Fig. 1a), are composed of moderately indurated illite-rich sedimentary strata with scattered tuff and bentonitic marl (e.g., Neef, 1999; Browne, 2004; Maison et al., 2018; McArthur et al., 2020). Rivers in the area (e.g., the Waipaoa River, Fig. 1a) erode into poorly indurated Miocene-Pliocene sediments (Erdman & Kelsey, 1992; Reid, 1998; Browne, 2004; Marsaglia et al., 2010). Although smectite is also a reported constituent of the mudstones (Claridge, 1960), illite is the dominate clay in soil samples from steep-land fields (Officer et al., 2006). Those watersheds (e.g., Waipaoa) generate unusually high yields of suspended sediment (Hicks et al., 2011), and discharge should supply the Hikurangi shelf and slope with illite-rich clays.

Sedimentologists usually attribute high concentrations of smectite to weathering or alteration of volcanic sources (Biscaye, 1965; Hein & Scholl, 1978; Fagel, 2007; Huff, 2016). The East Cape region of North Island (Fig. 1) exposes several potential parents for detrital smectite. Mafic mélange (disrupted ophiolite) and small lenses of volcanic conglomerate do exist in the East Coast Allochthon (Brothers & Delaloye, 1982; Cluzel et al., 2010; Marsaglia et al., 2014), but their exposures are probably not large enough to produce all the smectite we found in the slope muds. The Taupo Volcanic Zone (TVZ), on the other hand, fits all the prerequisites for a regionally extensive source (Fig. 1a), with enormous andesitic to rhyolitic calderas (Kohn & Topping, 1978; Cole et al., 2014; Wilson & Rowland, 2016), ignimbrites, tephras, and lahars (e.g., Cronin et al., 1999; Hidgson & Manville, 1999; Lowe et al., 2013; Downs et al., 2014; Procter et al., 2014; Gravley et al., 2016). Their chemical weathering products are demonstrably smectite-dominant, and those clays are ubiquitous in geothermal and hydrothermal systems (Libbey et al., 2013; Simpson et al., 2019; Heap et al., 2020). After reaching the Bay of Plenty coast, at least some particulates from the TVZ are likely swept eastward by the East Cape Current before that current bifurcates around East Cape and directs suspensions toward the SW (Fig. 1a). Moreover, heavily weathered tephra is widespread in coastal exposures around the Bay of Plenty (Iso et al., 1982), and smectite alteration of volcaniclastic sediment permeates into geothermal systems offshore (Hocking et al., 2010). Farther to the east near East Cape, discharge from the Waiapu River is known to contain remarkably high loads of suspended sediment (Hicks et al., 2011); that discharge might contribute some

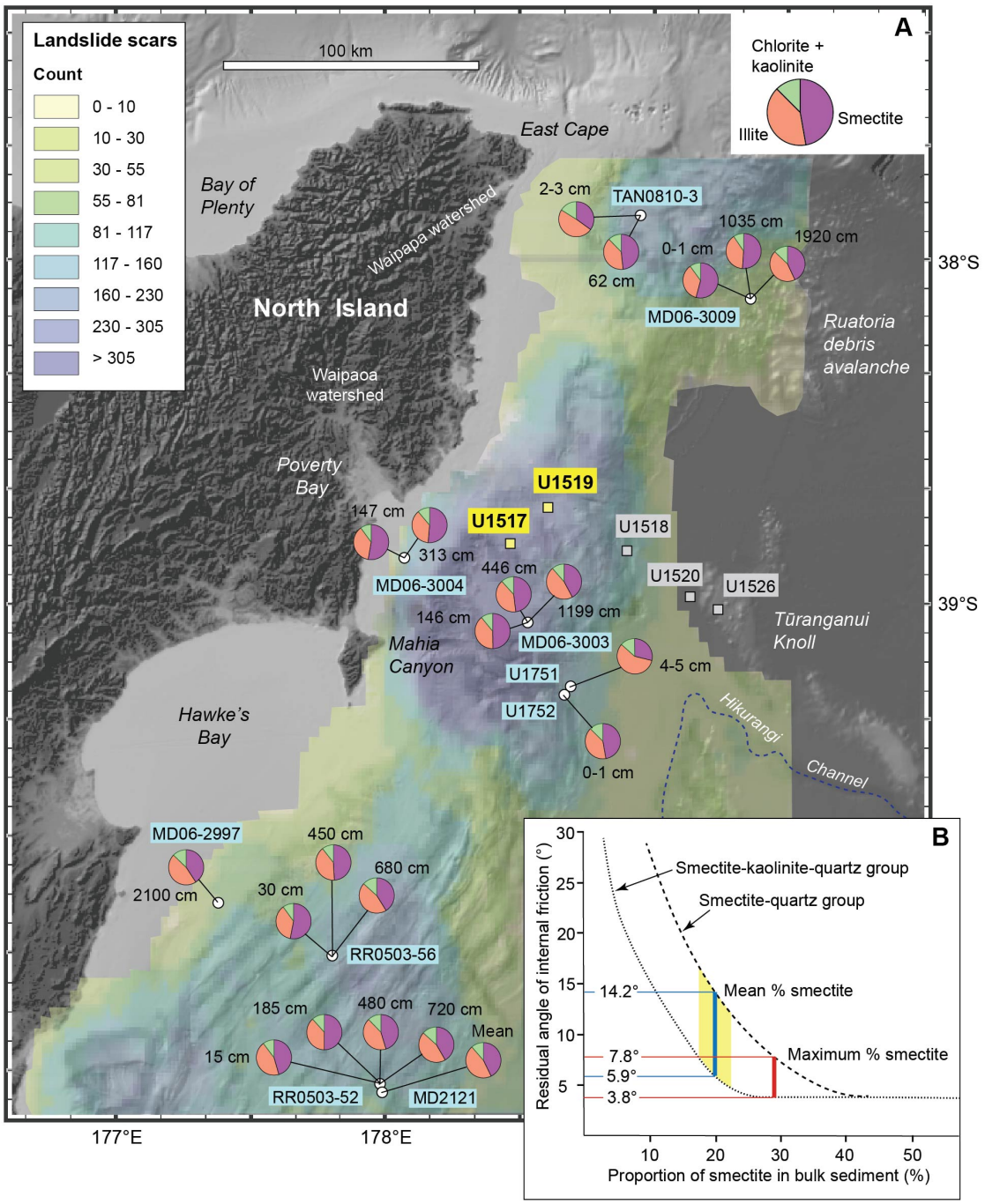

Figure 3a. Locations of piston-gravity cores used in this study, with depths of specimens in cm below seafloor (Underwood, 2020). Pie diagrams depict normalized proportions of smectite, illite, and undifferentiated (chlorite + kaolinite). Background shows frequency distribution of landslide scars (from Watson et al., 2020). 3b. Empirical relation between proportion of smectite in bulk sediment and residual angle of internal friction, as determined by Tiwari & Marui (2005). Average and maximum values for Site U1517 yield predictions for the Tuaheni landslide. Yellow field depicts one standard deviation around the mean.

additional smectite into suspensions carried by the East Cape Current, but also higher concentrations of illite and chlorite liberated from easily eroded sedimentary strata. We suggest that the typical Hikurangi clay

mineral assemblage, with appreciable amounts of both smectite and illite, is a product of blending among suspensions from multiple sources along the pathway of the East Cape Current.

4.2. Implications for Slope Stability

It seems certain that several factors combine to destabilize the Hikurangi trench slope, but it is challenging to isolate and quantify the impact of each. Rapid accumulation of low-permeability sediments often contributes to overpressured conditions on continental slopes (e.g., Stoecklin et al., 2017). Contourite drifts elsewhere are known to be susceptible to failure due to such factors as localized oversteepening of the seafloor, scouring by currents, and/or pronounced climate-induced changes of lithology (e.g., Laberg et al., 2016; Prieto et al., 2016; Miramontes et al., 2018; Gatter et al., 2020). Fluid pressures in such deposits can be exacerbated by trapping or seepage of free gas (e.g., Faure et al., 2006; Gross et al., 2018; Crutchley et al., 2022). The Hikurangi margin, in addition, has a propensity for moderate to large subduction-induced earthquakes (Dowrick & Rhoades, 1998; Cubrinovski et al., 2022), so it is also logical to expect dynamic loading during seismic shaking, together with transient increases of fluid pressure (e.g., Stegmann et al., 2007). The Ruatoria avalanche offshore North Island has been attributed to seamount subduction (Collot et al., 2001; Lewis et al., 2004). No matter how sedimentologists might debate interpretations of detrital provenance and routing paths for any depositional system, the abundance of clay and the composition of clay minerals also play key roles in modulating sediment's frictional strength. Smectite is widely regarded as a crucial ingredient in that sense (Tembe et al., 2010). Residual shear strength decreases dramatically once the proportion of smectite exceeds 25–30% of the bulk mineralogy (e.g., Luipini et al., 1981; Logan & Rauenzahn, 1987). The results of Tiwari & Marui (2005) allow us to predict ranges of residual shear strength for the Tuaheni landslide based on our calculated percentages of smectite in the bulk sediment. Using the empirical relation for two-component quartz-smectite mixtures, those %-smectite values translate to predicted angles of internal friction that range from an average of 14.2° to a minimum of 7.8° (Fig. 3b). The three-component quartz-smectite-kaolinite group (Tiwari & Marui, 2005) provides a more realistic match for Hikurangi bulk sediment. Using that curve, our calculated values for bulk %-smectite translate to predictions of 5.9° for the average and only 3.8° for the minimum angle of internal friction (Fig. 3b). Accordingly, although direct tests of frictional property are warranted to verify, we stipulate that clay composition preconditions the Tuaheni strata to fail without having a preferred slip surface along any layer-specific weak interval.

Crutchley et al. (2022) contended that the basal shear zone of the Tuaheni slide exploited a stratigraphic interval with comparatively low shear strength (i.e., a pre-existing weak layer). Weak layers are known to occur in many lithologies (Gatter et al., 2021). Some weak layers evidently predate failure and function as the preferred glide planes, whereas others form during failure events due to realignment of grain fabric (Locat et al., 2014; Gatter et al., 2021). In some instances, contrasts of hydrogeologic properties across a pronounced lithologic boundary allow pore pressure to build up along a potential failure plane (e.g., Stegmann et al., 2007).

Elsewhere, tephra beds act as weak layers; their suggested causes include fabric rearrangement and volume reduction during shearing (Harders et al., 2010), alteration of the volcanic glass to smectite (Miramontes et al., 2018), or the tephra's role in focusing transient perturbations of pore-fluid pressure (Wiemer et al., 2015; Kuhlmann et al., 2016). Our data allow for tests of those possibilities.

Surprisingly, we found no evidence at Site U1517 for pronounced compositional variations within or across any of the weak layers or inferred slip surfaces. Compositional homogeny prevails across the slip surface at ~41 mbsf, across the base of the creeping slide interval (as defined by seismic-reflection data at ~59 mbsf), and within the weak layer at ~31 mbsf (Fig. 2a). None of those intervals in the cores coincides with a layer of volcanic ash, or unusually high amounts of total clay, or unusually high concentrations of smectite (Fig. 3a). Instead, we see a subtle facies transition between mud with stacked couplets of silt and mud (unit III) and mostly mud (unit IV). That facies change probably resulted from temporal variations in sediment supplies and current strength. The weak layer at ~31 mbsf occurs in the middle of unit III, without any obvious facies change or anomaly in sediment texture, internal sedimentary structures, bed thickness, or bed geometry (Fig. 2a). That weak layer probably developed during a slip event via realignment of phyllosilicate grain fabric (Crutchley et al., 2022).

If we accept the validity of the East Cape Current as the path for routing residual smectite toward the SW, then it follows for slope stability offshore North Island to improve "downstream" where more detrital illite and chlorite enters the dispersal system from the Waipaoa and kindred watersheds (Fig. 1a). XRD data from piston/gravity cores are consistent with that interpretation (Fig. 3a). The frequency of landslide scars decreases where proportions of illite and chlorite are higher (Watson et al., 2020). In the opposite direction, landslide scars are more concentrated in areas that are closer to the volcanic sources of smectite-rich clay (Fig. 3a).

5 Conclusions

Our results reinforce the notion that submarine slopes fail in response to many interwoven variables, including mineralogy, and those variables combine in ways that are unique to each individual landslide. The homogeny of mud across the Hikurangi trench slope is a result of strong currents blending suspensions from multiple sources. Smectite is the most abundant clay mineral, with concentrations high enough to reduce the bulk mud's angle of internal friction to an average of ~6° and a minimum of ~4°. We did not find compositional excursions along any inferred slip surfaces or weak layers within the Tuaheni landslide. Smectite abundance and slide scars both decrease toward the SW, in the "downstream" direction of the East Cape Current. Thus, sediment-dispersal systems such as Hikurangi can contribute inconspicuously to strike-parallel changes in slope instability by modulating composition. Our study demonstrates why quantitative analyses of mineralogy

should be included in any holistic investigation of landslides, to test for possible compositional preconditioning.

Acknowledgments

This study used samples provided by the International Ocean Discovery Program (IODP) and core repositories at Lamont-Doherty Earth Observatory, Oregon State University (supported by NSF Grant number OCE-1558679), and the New Zealand National Institute of Water and Atmospheric Research. Funding was provided by the U.S. Science Support Program and, for piston/gravity cores, by a grant to Laura Wallace at GNS Science of New Zealand. We thank the crew members on JOIDES Resolution, IODP technicians, and fellow shipboard scientists for assisting with sample acquisition. Karissa Rosenberger and Mercedes Salazar helped with sample preparation, and Kelsey McNamara completed XRD scans at the New Mexico Bureau of Geology and Mineral Resources.

Open Research

Tabulations of XRD data, descriptions of methods, and error analysis are accessible in data reports distributed by the International Ocean Discovery Program: https://doi.org/10.14379/iodp.proc.372B375.201.2020; https://doi.org/10.14379/iodp.proc.372B375.203.2020; https://doi.org/10.14379/iodp.proc.372B375.209.2022; https://doi.org/10.14379/iodp.proc.372A.201.2021

References

Alexander, C. R., Walsh, J. P., & Orpin, A. R. (2010). Modern sediment dispersal and accumulation on the outer Poverty continental margin. *Marine Geology*, 270, 213–226. doi:10.1016/j.margeo.2009.10.015

Alonso, B., Ercilla, G., Casas, D., Stow, D.A.V., Rodriguez-Tovar, F. J., Dorador, J., & Hernandez-Molina, F.-J. (2016). Contourite vs gravity-flow deposits of the Pleistocene Faro Drift (Gulf of Cadiz): Sedimentological and mineralogical approaches. *Marine Geology*, 377, 77–94. http://dx.doi.org/10.1016/j.margeo.2015.12.016

Baeten, N. J., Laberg, J. S., Vanneste, M., Forsberg, C. F., Kvalstad, T. J., Forwick, M., Vorren, T. O., & Hafildason, H. (2014). Origin of shallow submarine mass movements and their glide planes – Sedimentological and geotechnical analyses from the continental slope off northern Norway. *Journal of Geophysical Research, Earth Surface*, 119. doi:10.1002/2013JF003068

Bailey, W. S., McArthur, A. D., & McCaffrey, W.D. (2020). Distribution of contourite drifts on convergent margins: Examples from the Hikurangi subduction margin of New Zealand. *Sedimentology*, 67, 12779. doi:10.1111/sed.12779

Bailey, W., McArthur, A., & McCaffrey, W. (2021). Sealing potential of contourites drifts in deep-water fold and thrust belts: Examples from the Hikurangi Margin, New Zealand. *Marine Petroleum Geology*, 123, 104776. https://doi.org/10.1016/j.marpetgeo.2020.104776

Barnes, P. M., Nicol, A., and Harrison, T. (2002). Late Cenozoic evolution and earthquake potential of an active listric thrust complex above the Hikurangi subduction zone, New Zealand. *Geological Society of America Bulletin*, 114(11), 1379–1405.

Barnes, P. M., Pecher, I., & LeVay, L. (2017). *Expedition 372 scientific prospectus: creeping gas hydrate slides and LWD for Hikurangi subduction margin*. College Station, TX: International Ocean Discovery Program. http://dx.doi.org/10.14379/iodp.sp.372.2017

Barnes, P. M., Pecher, I. A., LeVay, L. J., & 34 others (2019a). Site U1517. In I. A. Pecher, P. M. Barnes, L. J. LeVay, Expedition 372A Scientists (Eds.), *Proceedings of the International Ocean Discovery Program* (Vol. 372A). College Station, TX: International Ocean Discovery Program. https://doi.org/10.14379/iodp.proc.372A.103.2019

Barnes, P. M., Wallace, L. M., Saffer, D. M., Pecher, I. A., Petronotis, K. E., LeVay, L. J., and 55 others (2019b). Site U1519. In L. M. Wallace, D. M. Saffer, P. M. Barnes, I. A. Pecher, K. E. Petronotis, L. J. LeVay, Expedition 372/375 Scientists (Eds.), *Hikurangi Subduction Margin Coring, Logging, and Observatories*. *Proceedings of the International Ocean Discovery Program* (Vol. 372B/375). College Station, TX: International Ocean Discovery Program. https://doi.org/10.14379/iodp.proc.372B375.104.2019

Bartetzko, A., & Kopf, A. J. (2007). The relationship of undrained shear strength and porosity with depth in shallow (<50 m) marine sediments. *Sedimentary Geology*, 196, 235–249. doi:10.1016/j.sedgeo.2006.04.005

Biscaye, P. E. (1965). Mineralogy and sedimentation of recent deep-sea clay in the Atlantic Ocean and adjacent seas and oceans. *Geological Society of America Bulletin*, 76, 803–832.

Bostock, H., Jenkins, C., Mackay, K., Carter, L., Nodder, S., & Orpin, A. (2018). Distribution of surficial sediments in the ocean around New Zealand/Aotearoa. Part A: continental slope and deep ocean. *New Zealand Journal of Geology and Geophysics*, 62(1), 1–23. https://doi.org/10.1080/00288306.2018.1523198

Bourget, J., Zaragosi, S., Ellouz-Zimmermann, N., Mouchot, N., Garlan, T., Schneider, J.-L., Lanfumey, V., & Lallemant, S. (2011). Turbidite system architecture and sedimentary processes along topographically complex slopes: the Makran convergent margin. *Sedimentology*, 58, 376–406. doi:10.1111/j.1365-3091.2010.01168.x

Brothers, R. N., & DeLaloye, M. (1982). Obducted ophiolites of North Island, New Zealand: origin, age, emplacement and tectonic implications for Tertiary and Quaternary volcanicity. *New Zealand Journal of Geology and Geophysics, 25, 257–274*.

Browne, G.H. (2004). Late Neogene sedimentation adjacent to the tectonically evolving North Island axial ranges: insights from Kuripapango, western Hawke's Bay. *New Zealand Journal of Geology and Geophysics*, 47, 663–674.

Carter, L., & McCave, I. N. (1997). The sedimentary regime beneath the Deep Western Boundary Current inflow to the southwest Pacific Ocean. *Journal of Sedimentary Research*, 67(6), 1005–1017.

Carter, L., & McCave, I. N. (2002). Eastern New Zealand drifts, Miocene-Recent. In D. A. V. Stow, C. J. Pudsey, J. A. Howe, J.-C. Faugeres, A. R. Viana (Eds.). *Deep-water contourite systems: Modern drifts and ancient series, seismic and sedimentary characteristics* (Memoir 22, pp. 385–407). London, Geological Society.

Carter, L., & Wilkin, J. (1999). Abyssal circulation around New Zealand – a comparison between observations and a global circulation model. *Marine Geology*, 159, 221–239.

Carter, L., Carter, R. M., & McCave, I. N. (2004). Evolution of the sedimentary system beneath the deep Pacific inflow off eastern New Zealand. *Marine Geology*, 205, 9–27. doi:10.1016/S0025-3227(04)00016-7

Chiswell, S. M. (2000). The Wairarapa Coastal Current. *New Zealand Journal of Marine and Freshwater Research*, 34, 303–315.

Chiswell, S. M. (2005). Mean and variability in the Wairarapa and Hikurangi Eddies, New Zealand. *New Zealand*

Journal of Marine and Freshwater Research, 39, 121–134.

Chiswell, S. M., & Roemmich, D. (1998). The East Cape Current and two eddies: a mechanism for larval retention? *New Zealand Journal of Marine and Freshwater Research*, 32, 385–397.

Chiswell, S. M., Bostock, H. C., Sutton, P. J. H., & Williams, J. M. (2015). Physical oceanography of the deep seas around New Zealand: a review. *New Zealand Journal of Marine and Freshwater Research*, 49(2), 286–317. doi:10.1080/00288330.2014.992919

Claridge, G. G. C. (1960). Clay minerals, accelerated erosion, and sedimentation in the Waipaoa River catchment. *New Zealand Journal of Geology and Geophysics,* 3, 184–191.

Cluzel, D., Black, P. M., Picard, C., & Nicholson, K. N. (2010). Geochemistry and tectonic setting of Matakaoa Volcanics, East Coast Allochthon, New Zealand: Suprasubduction zone affinity, regional correlations, and origin. *Tectonics*, 29, TC2013. doi:10.1029/2009TC002454

Cole, J. W., Deering, C. D., Burt, R. M., Sewell, S., Shane, P. A. R., & Matthews, N. E. (2014). Okataina Volcanic Center, Taupo Volcanic Zone, New Zealand: A review of volcanism and synchronous pluton development in a active, dominantly silicic caldera system. *Earth Science Reviews*, 128, 1–17. http://dx.doi.org/10.1016/j.earscirev.2013.10.008

Collot, J.-Y., Lewis, K., Lamarche, G., & Lallemand, S. (2001). The giant Ruatoria debris avalanche on the northern Hikurangi margin, New Zealand: Result of oblique seamount subduction. *Journal of Geophysical Research*, 106(B9), 19,271–19,297.

Contardo, X., Cembrano, J., Jensen, A., & Diaz-Naveas, J. (2008). Tectono-sedimentary evolution of marine slope basins in the Chilean forearc (33°30'–36°50'S): Insights into their link with the subduction process. *Tectonophysics*, 459, 206–218. doi:10.1016/j.tecto.2007.12.014

Contardo, X. J., Kukowski, N., & Cembrano, J. M. (2011). Material transfer and its influence on the formation of slope basins along the South Central Chilean convergent margin: Insights from scaled sandbox experiments. *Tectonophysics*, 513, 20–36. doi:10.1016/j.tecto.2011.09.016

Couvin, B., Georgiopoulou, A., Mountjoy, J. J., Amy, L., Crutchley, G. J., Brunet, M., et al. (2020). A new depositional model for the Tuaheni Landslide Complex, Hikurangi margin, New Zealand. In A. Georgiopoulous et al. (Eds.). *Subaqueous mass movements and their consequences: Advances in process understanding, monitoring and hazard assessments*, *Special Publication* (Vol. 500, pp. 551–566). London, Geological Society. https://doi.org/10.1144/SP500-2019-180

Cronin, S. J., Neall, V. E., Lecointre, J. A., & Palmer, A. S. (1999). Dynamic interactions between lahars and stream flow: A case study from Ruapehu volcano, New Zealand. *Geological Society of America Bulletin*, 111(1), 28–38.

Crutchley, G. J., Geiger, S., Pecher, I. A., Gorman, A. R., Zhu, H., & Henrys, S. A. (2010). The potential influence of shallow gas and gas hydrates on seafloor erosion of Rock Garden, an uplifted ridge offshore of New Zealand. *Geo-Marine Letters*, 30, 283–303. doi:10.1007/s00367-010-0186-y

Crutchley, G. J., Elger, J., Kuhlmann, J., Mountjoy, J. J., Orpin, A., Georgiopoulou, A., et al. (2022). Investigating the basal shear zone of the submarine Tuaheni landslide complex, New Zealand: A core-log-seismic integration study. *Journal of Geophysical Research: Solid Earth*, 127, e2021JB021997. https://doi.org/10.1029/2021JB021997

Cubrinovski, M., Bradley, B. A., Wentz, F., & Balachandra, A. (2022). Re-evaluation of New Zealand seismic hazard for geotechnical assessment and design. *Bulletin New Zealand Society for Earthquake Engineering*, 55(1), 1–14.

de Castro, S., Hernandez-Molina, F. J., de Weger, W., Jimenez-Espejo, F. J., Rodriguez-Tovar, F. J., Mena, A., Llave, E., & Sierro, F. J. (2020). Contourite characterization and its discrimination from other deep-water deposits in the Gulf of Cadiz contourite depositional system. *Sedimentology*. doi:10.1111/sed.12813

Ding, F., Spiess, V., Fekete, N., Murton, B., Bruning, M., & Bohrmann, G. (2010). Interaction between accretionary thrust faulting and slope sedimentation at the frontal Makran accretionary prism and its implications for hydrocarbon seepage. *Journal of Geophysical Research*, 115, B08106. doi:10.1029/2008JB006246

Downs, D. T., Wilson, C. J. N., Cole, J. W., Rowland, J. V., Calvert, A. T., Leonard, G. S., & Keall, J. M. (2014). Age and eruptive center of the Paeroa Subgroup ignimbrites (Whakamaru Group) within the Taupo Volcanic Zone of New Zealand. *Geological Society of America Bulletin*, 126(9/10), 1131–1144. doi:10.1130/B30891.1

Dowrick, D. J., & Rhoades, D. A. (1998). Magnitudes of New Zealand earthquakes, 1901–1993. *Bulletin New Zealand National Society for Earthquake Engineering*, 31(4), 260–280.

Ellis, S., Pecher, I., Kukowski, N., Xu, W., Henrys, S., & Greinert, J. (2010). Testing proposed mechanisms for seafloor weakening at the top of gas hydrate stability on an uplifted submarine ridge (Rock Garden), New Zealand. *Marine Geology*, 272, 127–140. doi:10.1016/j.margeo.2009.10.008

Erdman, C.F., & Kelsey, H. M. (1992). Pliocene and Pleistocene stratigraphy and tectonics, Ohara Depression and Wakarara Range, North Island, *New Zealand Journal of Geology and Geophysics*, 35, 177–192.

Fagel, N. (2007). Clay minerals, deep circulation and climate. In C. Hillaire-Marcel & A. De Vernal (Eds.), *Proxies in Late Cenozoic Paleoceanography* (pp. 139–184). Amsterdam, Elsevier.

Faure, K., Greinert, J., Pecher, I. A., Graham, I. J., Massoth, G. J., de Ronde, C. E., Wright, I. C., Baker, E. T., & Olson, E. J. (2006). Methane seepage and its relation to slumping and gas hydrate at the Hikurangi margin, New Zealand. *New Zealand Journal of Geology and Geophysics*, 49, 503–516.

Foster, G., & Carter, L. (1997). Mud sedimentation on the continental shelf at an accretionary margin – Poverty Bay, New Zealand. *New Zealand Journal of Geology and Geophysics*, 40, 157–173.

Gatter, R., Clare, M. A., Hunt, J. E., Watts, M., Madhusudhan, B. N., Tailing, P. J., & Huhn, K. (2020). A multi-disciplinary investigation of the AFEN Slide: the relationship between contourites and submarine landslides. In A. Georgiopoulous et al. (Eds.). *Subaqueous mass movements and their consequences: Advances in process understanding, monitoring and hazard assessments*, *Special Publication* (Vol. 500, pp. 173–193). London, Geological Society. https://doi.org/10.1144/SP500-2019-184

Gatter, R., Clare, M. A., Kuhlmann, J., & Huhn, K. (2021). Characterization of weak layers, physical controls on their global distribution and their role in submarine landslide formation. *Earth Science Reviews*, 223, 103845. https://doi.org/10.1016/j.earthscirev.2021.103845

Ghisetti, F. C., Barnes, P. M., Ellis, S., Piazza-Faverola, A. A., & Barker, D. H. N. (2016). The last 2 Myr of accretionary wedge construction in the central Hikurangi margin (North Island, New Zealand): Insights from structural modeling. *Geochemistry Geophysics Geosystems*, 17, 2661–2686. doi:10.1002/2016GC006341

Gorsline, D. S. (1984). A review of fine-grained sediment origins, characteristics, transport, and deposition. In D. A. V. Stow & D. J. W. Piper (Eds.), *Fine-grained sediments: Deep-water processes and facies*. *Special Publication* (Vol. 15, pp. 17–34). London, Geological Society.

Gravley, D. M., Deering, C. D., Leonard, G. S., & Rowland, J. V. (2016). Ignimbrite flare-ups and their drivers: A New Zealand perspective. *Earth Science Reviews*, 162, 65–82. http://dx.doi.org/10.1016/j.earscirev.2016.09.007

Gross, F., Mountjoy, J. J., Crutchley, G. J., Bottner, C., Koch, S., Bialas, J., et al. (2018). Free gas distribution and basal shear zone development in a subaqueous landslide – Insight from 3D seismic imaging of the Tuaheni

528 Landslide Complex, New Zealand. *Earth and Planetary Science Letters*, 502, 231–243.
529 https://doi.org/10.1016j.epsl.2018.09.002
530
531 Hampton, M. A., Lee, H. J ., & Locat, J. (1996). Submarine landslides. *Reviews in Geophysics*, 34(1), 33–59.
532
533 Harders, R., Kutterolf, S., Hensen, C., Moerz, T., & Brueckman, W. (2010). Tephra layers: A controlling factor on
534 submarine translational sliding? *Geochemistry Geophysics Geosystems*, 11(5), Q05S23.
535 doi:10.1029/2009GC002844
536
537 Harders, R., Ranero, C. R., Weinrebe, W., & Behrmann, J. H. (2011). Submarine slope failures along the convergent
538 continental margin of the Middle America Trench. *Geochemistry Geophysics Geosystems*, 12(6), Q05S32.
539 doi:10.1029/2010GC003401
540
541 Heap, M. J., Gravley, D. M., Kennedy, B. M., Gilg, H. A., Bertolett, E., & Barker, S. L. L. (2020). Quantifying the
542 role of hydrothermal alteration in creating geothermal and epithermal mineral resources: The Okakuri ignimbrite
543 (Taupo Volcanic Zone, New Zealand). *Journal of Volcanology and Geothermal Research*, 390, 106703.
544 https://doi.org.10.1016/j.volgeores.2019.106703
545
546 Hein, J. R., & Scholl, D. W. (1978). Diagenesis and distribution of late Cenozoic volcanic sediment in the southern
547 Bering Sea. *Geological Society of America Bulletin*, 89(2), 197–210.
548
549 Hicks, D. M., Shankar, U., McKerchar, A. I., Basher, L., Lynn, I., Page, M., & Jessen, M. (2011). Suspended
550 sediment yields from New Zealand rivers. *Journal of Hydrology*, 50(1), 81–142.
551
552 Hidgson, K. A., & Manville, V. R. (1999). Sedimentology and flow behavior of a rain-triggered lahar,
553 Mangatoetoenui Stream, Ruapehu volcano, New Zealand. *Geological Society of America Bulletin*, 111(5), 743–754.
554
555 Hill, J. C., Watt, J. T., Brothers, D. S., & Kluesner, J. W. (2020). Submarine canyons, slope failures and mass
556 transport processes in southern Cascadia. In A. Georgiopoulous et al. (Eds.). *Subaqueous mass movements and their*
557 *consequences: Advances in process understanding, monitoring and hazard assessments*, *Special Publication* (Vol.
558 500, pp. 453–475). London, Geological Society. https://doi.org/10.1144/SP500-2019-169
559
560 Hocking, M. W. A., Hannington, M. D., Percival, J. B., Stoffers, P., Schwarz-Schampera, U., & de Ronde, C. E. J.
561 (2010). Clay alteration of volcaniclastic material in a submarine geothermal system, Bay of Plenty, New Zealand.
562 *Journal of Volcanology and Geothermal Research*, 191, 180–192. doi:10.1016/j.volgeores.2010.01.018
563
564 Huff, W. D. (2016). K-bentonites: A review. *American Mineralogist*, 101, 43–70. http://dx.doi.org/10.2138/am-
565 2016-5339
566
567 Ikari, M. J., Saffer, D. M., & Marone, C. (2007). Effect of hydration state on the frictional properties of
568 montmorillonite-based fault gouge. *Journal of Geophysical Research*, 112, B06423. doi:10.1029/2006JB004748
569
570 Ikari, M. J., Strasser, M., Saffer, D. M., & Kopf, A. J. (2011). Submarine landslide potential near the megasplay
571 fault at the Nankai subduction zone. *Earth and Planetary Science Letters*, 312, 453–462.
572 doi:10.1016/j.epsl.2011.10.024
573
574 Ikari, M. J., Kopf, A.J., Hupers, A., & Vogt, C. (2018). Lithologic controls on frictional strength variations in
575 subduction zone sediment inputs. *Geosphere*, 14(2), 604–625. doi:10.1130/GES01546.1
576
577 Iso, N., Okada, A., Ota, Y., & Yoshikawa, T. (1982). Fission-track ages of late Pleistocene tephra on the Bay of
578 Plenty coast, North Island, New Zealand. *New Zealand Journal of Geology and Geophysics*, 25, 295–303.
579
580 Jiao, R., Seward, D., Little, T. A., & Kohn, B. P. (2014). Thermal history and exhumation of basement rocks from
581 Mesozoic to Cenozoic subduction cycles, central North Island, New Zealand. *Tectonics*, 33, 1920–1935.
582 doi:10.1002/2014TC003653
583

584 Kock, I., & Huhn, K. (2007). Influence of particle shape on the frictional strength of sediments – A numerical case
585 study. *Sedimentary Geology*, 196, 217–233. doi:10.1016/j.sedgeo.2006.07.011
586
587 Kohn, B. P., & Topping, W. W. (1978). Time-space relationships between late Quaternary rhyolitic and andesitic
588 volcanism in the southern Taupo volcanic zone, New Zealand. *Geological Society of America Bulletin*, 89(8), 1265–
589 1271.
590
591 Kremer, K., Usman, M. O., Satoguchi, Y., Nagahashi, Y., Vadkkepuliyambatta, S., Panieri, G., & Strasser, M.,
592 (2017). Possible climate preconditioning on submarine landslides along a convergent margin, Nankai Trough (NE
593 Pacific). *Progress in Earth and Planetary Science*, 4, 20. doi:10.1186/s40645-017-0134-9
594
595 Kuhlman, J., Huhn, K., & Ikari, M. J., (2016). Do embedded volcanoclastic layers serve as potential glide planes?:
596 An integrated analysis from the Gela Basin offshore southern Sicily. In G. Lamarche, G., et al. (Eds.), *Submarine*
597 *mass movements and their consequences, advances in natural and technological hazards research* (Vol. 41, pp.
598 273–280). Switzerland, Springer International Publishing. doi:10.1007/978-3-319-20979-1_27
599
600 Kuhlmann, J., Orpin, A. R., Mountjoy, J. J., Crutchley, G. J., Henrys, S., Lunenburg, R., & Huhn, K. (2019).
601 Seismic and lithofacies characterization of a gravity core transect down the submarine Tuaheni Landslide Complex,
602 NE New Zealand. In D. G. Lintern (Eds.), *Subaqueous mass movements, Special Publications* (Vol. 477, pp. 479–
603 495). London, Geological Society. https://doi.org/10.1144/SP477.37
604
605 Laberg, J. S., Baeten, N. J., Vanneste, M., Forsberg, C. F., Forwick, M., & Haflidason, H. (2016). Sediment failure
606 affecting muddy contourites on the continental slope offshore northern Norway: Lessons learned and some
607 outstanding issues. In G. Lamarche et al. (Eds.), *Submarine mass movements and their consequences, Advances in*
608 *natural and technological hazards research* (Vol. 41, pp. 281–290). Switzerland, Springer International Publishing.
609 doi:10.1007/978-3-319-20979-1_28
610
611 Lewis, K. B., Lallemand, S. E., & Carter, L. (2004). Collapse in a Quaternary shelf basin off East Cape, New
612 Zealand: evidence for passage of a subducted seamount inboard of the Ruatoria giant avalanche. *New Zealand*
613 *Journal of Geology and Geophysics,* 47, 415–429.
614
615 Libbey, R. B., Longstaffe, F. J., & Flemming, R. L. (2013). Clay mineralogy, oxygen isotope geochemistry, and
616 water/rock ratio estimates, Te Mihi area, Wairakei geothermal field, New Zealand. *Clays and Clay Minerals*, 61(3),
617 204–217. doi:10.1346/CCMN.2013.0610304
618
619 Locat, J., & Lee, H. J. (2002). Submarine landslides: advances and challenges. *Canadian Geotechnical Journal*, 39,
620 193–212. doi:10.1139/T01-089
621
622 Locat, J., Leroueil, S., Locat, A., & Lee, H. (2014). Weak layers: Their definition and classification from a
623 geotechnical perspective. In S. Krastel et al. (Eds.), *Submarine mass movements and their consequences, advances*
624 *in natural and technological hazards research* (pp. 3–12). Switzerland, Springer International Publ.
625 doi:10.1007/978-3-319-00972-8_1
626
627 Logan, J. M., & Rauenzahn, K. A. (1987). Frictional dependence of gouge mixtures of quartz
628 and montmorillonite on velocity, composition and fabric. *Tectonophysics*, 144, 87–108.
629
630 Lowe, D. J., Blaauw, M., Hogg, A. G., & Newnham, R. M. (2013). Ages of 24 widespread tephras erupted since
631 30,000 years ago in New Zealand, with re-evaluation of the timing and palaeoclimatic implications of the
632 Lateglacial cool episode recorded at Kaipo bog. *Quaternary Science Reviews*, 74, 170–194.
633 http://dx.doi.org/10.1016/j.quascirev.2012.11.022
634
635 Luo, M., Torres, M. E., Kasten, S., & Mountjoy, J. J. (2020). Constraining the age and evolution of the Tuaheni
636 Landslide Complex, Hikurangi margin, New Zealand, using pore-water geochemistry and numerical modeling.
637 *Geophysical Research Letters*, 47, e2020GL087243. https://doi.org/10.1029/2020GL087243
638
639 Lupini, J. F., Skinner, A. E., & Vaughan, P. R. (1981). The drained residual strength of cohesive

soils. *Geotechnique*, 31, 181–213.

MacKinnon, T. C. (1983). Origin of Torlesse terrane and coeval rocks, South Island, New Zealand. *Geological Society of America Bulletin*, 94, 967–985.

Maison, T., Potel, S., Malie, P., Ferreiro Mahlmann, R., Chanier, F., Mahieux, G., & Bailleul, J. (2018). Low-grade evolution of clay minerals and organic matter in fault zones of the Hikurangi prism (New Zealand). *Clay Minerals*, 53, 579–602. https://doi.org/10.1180/clm.2018.46

Marden, M., Mazengarb, C., Palmer, A., Berryman, K., & Rowan, D. (2008). Last glacial aggradation and postglacial sediment production from the non-glacial Waipaoa and Waimata catchments, Hikurangi margin, North Island, New Zealand. *Geomorphology*, 99, 404–419. doi:10.1016/j.geomorph.2007.12.003

Marsaglia, K. M., DeVaughn, A. M., James, D. E., & Marden, M. (2010). Provenance of fluvial terrace sediments within the Waipaoa sedimentary system and their importance to New Zealand source-to-sink studies. *Marine Geology*, 270, 84–93. doi:10.1016/j.margeo.2009.10.017

Marsaglia, K. M., Mortimer, N., Bender-Whitaker, C., Marden, M., & Mazengarb, C. (2014). Ophioliticalstic Ikungia igneous conglomerate (Early Miocene), North Island, New Zealand: evidence for an island source related to subduction initiation and deposition within a slump-generated submarine slope re-entrant. *New Zealand Journal of Geology and Geophysics,* 57(2), 219–235. http://dx.doi.org/10.1080/00288306.2014.898665

Masson, D. G., Harbitz, C. B., Wynn, R. B., Pedersen, G., & Lovholt, F. (2006). Submarine landslides: processes, triggers and hazard prediction. *Philosophical Transactions Royal Society A*, 364, 2009–2039. doi:10.1098/rsta.2006.1810

McAdoo, B. G., Capone, M. K., & Minder, J. (2004). Seafloor geomorphology of convergent margins: Implications for Cascadia seismic hazard. *Tectonics*, 23, TC6008. doi:10.1029/2003TC001570

McArthur, A. D., Claussmann, B., Bailleul, J., Clare, A., & McCaffrey, W. D. (2020). Variation in syn-subduction sedimentation patterns from inner to outer portions of deep-water fold and thrust belts: examples from the Hikurangi subduction margin of New Zealand. In J. A. Hammerstein, R. DiCuia, M. A. Cottam, G. Zamora, & R. W. H. Butler (Eds.). *Fold and thrust belts: structural style, evolution and exploration, Special Publication* (Vol. 490, pp. 285–310). London, Geological Society. https://doi.org/10.1144/SP490-2018-95

McCave, I. N. (1984). Erosion, transport and deposition of fine-grained marine sediments. In D. A. V. Stow & D. J. W. Piper (Eds.), *Fine-grained sediments: Deep-water processes and facies*. *Special Publication* (Vol. 15, pp. 35–70). London, Geological Society.

Micallef, A., Mountjoy, J.J., Krastel, S., Crutchley, G., & Koch, S. (2015). Shallow gas and the development of a weak layer in submarine spreading, Hikurangi margin (New Zealand). In G. Lamarche et al. (Eds.), *Submarine mass movements and their Consequences, advances in natural and technological hazards research* (Vol. 41, pp. 419–426). Switzerland, Springer International Publ. doi:10.1007/978-3-319-20979-1_42

Miramontes, E., Garziglia, S., Sultan, N., Jouet, G., & Cattaneo, A. (2018). Morphological control of slope instability in contourites: a geotechnical approach. *Landslides*, 15, 1085–1095. doi:10.1007/s10346-018-0956-6

Miramontes, E., Sultan, N., Garziglia, S., Joulet, G., Pelleter, E., & Cattaneo, A. (2018). Altered volcanic deposits as basal failure surfaces of submarine landslides. *Geology*, 46(7), 663–666. https://doi.org/10.1130/G40268

Moore, D. M., & Reynolds, R. C., Jr. (1989). Sample preparation techniques for clay minerals. In D. M. Moore & R. C. Reynolds, Jr. (Eds.), *X-ray diffraction and the identification and analysis of clay minerals* (pp. 179–201). New York, Oxford University Press.

Moore, G. F., & Karig, D. E. (1976). Development of sedimentary basins on the lower trench slope. *Geology*, 4, 693–697.

Mountjoy, J. J., Barnes, P. M., & Pettinga, J. R. (2009a). Morphostructure and evolution of submarine canyons across an active margin: Cook Strait sector of the Hikurangi margin, New Zealand. *Marine Geology*, 260, 45–68. doi:10.1016/j.margeo.2009.01.006

Mountjoy, J. J., McKean, J., Barnes, P. M., & Pettinga, J. R. (2009b). Terrestrial-style slow-moving earthflow kinematics in a submarine landslide complex. *Marine Geology*, 267, 114–127. doi:10.1016/j.margeo.2009.09.007

Mountjoy, J. J., Micallef, A., Stevens, C. L., & Stirling, M. W. (2014a). Holocene sedimentary activity in a non-terrestrially coupled submarine canyon: Cook Strait Canyon system, New Zealand. *Deep-Sea Research II*, 104, 120–133. http://dx.doi.org/10.1016/j.dsr2.2013.09.001

Mountjoy, J. J., Pecher, I., Henrys, S., Crutchley, G., Barnes, P. M., & Plaza-Faverola, A. (2014b). Shallow methane hydrate system controls ongoing, downslope sediment transport in a low-velocity active submarine landslide complex, Hikurangi margin, New Zealand. *Geochemistry Geophysics Geosystems*, 15, 4137–4156. doi:10.1002/2014GC005379

Mountjoy, J. J., Georgiopoulou, A., Chaytor, J., Clare, M. A., Gamboa, D., & Moernaut, J. (2020). Subaqueous mass movements in the context of observations of contemporary slope failure. In: A. Georgiopoulou et al. (Eds.), *Subaqueous mass movements and their consequences: Advances in process understanding, monitoring and hazard assessments, Special Publications* (Vol. 500, pp. 1–12). London, Geological Society. https://doi.org/10.1144/SP500-2019-237

Muck, M. T., & Underwood, M. B. (1990). Upslope flow of turbidity currents: A comparison among field observations, theory, and laboratory models. *Geology*, 18, 54–57.

Nakamura, S., Gibo, S., Egashira, K., & Kimura, S. (2010). Platy layer silicate minerals for controlling residual strength in landslide soils of different origins and geology. *Geology*, 38(8), 743–746. doi:10.1130/G30908.1

Neef, G. (1999). Neogene development of the onland part of the forearc in northern Wairarapa, North Island, New Zealand: a synthesis. *New Zealand Journal of Geology and Geophysics*, 42, 113–135.

Nelson, C. H., Escutia, C., Damuth, J. E., & Twichell, D. C., Jr. (2011). Interplay of mass-transport and turbidite-system deposits in different active tectonic and passive continental margin settings: External and local controlling factors. In R. C. Shipp, P. Weimer, & H. W. Posamentier (Eds.), *Mass-transport deposits in deepwater settings, Special Publication* (Vol. 96). Society for Sedimentary Geology. https://doi.org/10.2110/sepmsp.096.039

Nishida, N. (2016). Microstructure of muddy contourites from the Gulf of Cadiz. *Marine Geology*, 377, 110–117. http://dx.doi.org/10.1016/j.margeo.2015.08.017

Officer, S. J., Tillman, R. W., Palmer, A. S., & Whitton, J. S. (2006). Variability of clay mineralogy in two New Zealand steep-land topsoils under pasture. *Geoderma*, 132, 427–440. doi:10.1016/j.geoderma.2004.11.027

Orpin, A. R. (2004). Holocene sediment deposition on the Poverty-slope margin by the muddy Waipaoa River, East Coast New Zealand. *Marine Geology*, 209, 69–90. doi:10.1016/j.margeo.2004.06.001

Paquet, F., Proust, J.-N., Barnes, P. M., & Pettinga, J. R. (2009). Inner-forearc sequence architecture in response to climatic and tectonic forcing since 150 ka: Hawke's Bay, New Zealand. *Journal of Sedimentary Research*, 79, 97–124. doi:10.2110/jsr.2009.019

Pedley, K. L., Barnes, P. M., Pettinga, J. R., & Lewis, K. B. (2010). Seafloor structural geomorphic evolution of the accretionary frontal wedge in response to seamount subduction, Poverty Indentation, New Zealand. *Marine Geology*, 270, 119–138. doi:10.1016/j.margeo.2009.11.006

Piper, D. J. W., von Huene, R., & Duncan, J. R. (1973). Late Quaternary sedimentation in the active eastern Aleutian Trench. *Geology*, 1(1), 19-–22.

Pouderoux, H., Proust, J.-N., Lamarche, G., Orpin, A., & Neil, H. (2012). Postglacial (after 18 ka) deep-sea sedimentation along the Hikurangi subduction margin (New Zealand): Characterisation, timing and origin of turbidites. *Marine Geology*, 295–298, 51–76. doi:10.1016/j.margeo.2011.11.002

Prieto, M. L., Moscardelli, L., & Wood, L. J. (2016). Exploring the influence of deepwater currents as potential triggers for slope instability. In G. Lamarche et al. (Eds.), *Submarine mass movements and their consequences, Advances in natural and technological hazards research* (Vol. 41, pp. 331–340). Switzerland, Springer International Publishing. doi:10.1007/978-3-319-20979-1_33

Procter, J. N., Cronin, S. J., Zernack, A. V., Lube, G., Stewart, R. B., Nemeth, K., & Keys, H. (2014), Debris flow evolution and the activation of an explosive hydrothermal system; Te Maari, Tongariro, New Zealand. *Journal of Volcanology and Geothermal Research*, 286, 303–316. http://dx.doi.org/10.1016/j.volgeores.2014.07.006

Reid, C. M. (1998). Stratigraphy, paleontology, and tectonics of lower Miocene rocks in the Waipatik/Mangatuna area, southern Hawke's Bay, New Zealand. *New Zealand Journal of Geology and Geophysics*, 41, 115–131.

Rodriguez-Tovar, F. J., & Hernandez-Molina, F. J. (2018). Ichnological analysis of contourites: Past, present and future. *Earth Science Reviews*. https://doi.org.1016/j.earscirev.2018.05.008

Saffer, D. M., Wallace, L. M., Barnes, P. M., Pecher, I. A., Petronotis, K. E., LeVay, L. J., and 55 others (2019). Expedition 372B/375 summary. In L. M. Wallace, D. M. Saffer, P. M. Barnes, I. A. Pecher, K. E. Petronotis, L. J. LeVay, Expedition 372/375 Scientists (Eds.), *Hikurangi subduction margin coring, logging, and observatories, Proceedings of the International Ocean Discovery Program* (Vol. 372B/375). College Station, TX, International Ocean Discovery Program. https://doi.org/10.14379/iodp.proc.372B375.101.2019

Screaton, E. J., Torres, M. E., Dugan, B., Heeschen, K. U., Mountjoy, J. J., Ayres, C., et al. (2019). Sedimentation controls on methane-hydrate dynamics across glacial/interglacial stages: An example from International Ocean Discovery Program Site U1517, Hikurangi margin. *Geochemistry Geophysics Geosystems*, 20. https://doi.org/10.1029/2019GC008603

Shimamoto, T., & J. M. Logan (1981). Effects of simulated clay gouges on the sliding behavior of Tennessee sandstone. *Tectonophysics, 75*, 243–255.

Silver, M. M. W., & Dugan, B. (2020). The influence of clay content on submarine slope failure: insights from laboratory experiments and numerical models. In A. Georgiopoulous et al. (Eds.). *Subaqueous mass movements and their consequences: Advances in process understanding, monitoring and hazard assessments. Special Publication* (Vol. 500, pp. 301–309). London, Geological Society. https://doi.org/10.1144/SP500-2019-186

Simpson, M. P., Gazley, M. F., Stuart, A. G. J., Pearce, M. A., Birchall, R., Chappell, D., et al. (2019). Hydrothermal alteration at the Karangahake epithermal Au-Ag deposit, Hauraki goldfield, New Zealand. *Economic Geology*, 114(2), 243–273. doi:10.5382/econgeo.2019.4630

Sporli, K. B. (1979). Mesozoic tectonics, North Island, New Zealand. *Geological Society of America Bulletin*, 89, 415–425.

Stegmann, S., Strasser, M., Anselmetti, F., & Kopf, A. (2007). Geotechnical in situ characterization of subaquatic slopes: The role of pore pressure transients versus frictional strength in landslide initiation. *Geophysical Research Letters*, 34, L07607. doi:10.1029/2006GL029112

Stoecklin, A., Friedli, B., & Puzrin, A. M. (2017). Sedimentation as a control for large submarine landslides: Mechanical modeling and analysis of the Santa Barbara Basin. *Journal of Geophysical Research: Solid Earth*, 122, 8645–8663. https://doi.org/10.1002/2017JB014752

Stow, D., & Smillie, Z. (2020). Distinguishing between deep-water sediment facies: turbidites, contourites and hemipelagites. *Geosciences*, 10, 68. doi:10.3390/geosciences10020068

Stow, D. A., Faugeres, J. C., Howe, J. A., Pudsey, C. J., & Viana, A. R. (2002). Bottom currents, contourites and deep-sea sediment drifts: current state-of-the-art. *Geological Society of London Memoir*, 22, 7–20.

Sultan, N., Cochonat, P., Canals, M., Cattaneo, A., Dennielou, B., Haflidason, H., et al. (2004). Triggering mechanisms of slope instability processes and sediment failures on continental margins: a geotechnical approach. *Marine Geology*, 213, 291–321. doi:10.1016/j.margeo.2004.10.011

Takahashi, M., Azuma, S., Ito, H., Kanagawa, K., & Inoue, A. (2014). Frictional properties of the shallow Nankai Trough accretionary sediments dependent on the content of clay minerals. *Earth Planets Space*, 66, 75. http://www.earth-planets-space.com/content/66/1/75

Tembe, S., Lockner, D. A., & Wong, T.-F. (2010). Effect of clay content and mineralogy on frictional sliding behavior of simulated gouges: Binary and ternary mixtures of quartz, illite, and montmorillonite. *Journal of Geophysical Research*, 115, B03416. doi:10.1029/2009JB006383

Tiwari, B., & Marui, H. (2005). A new method for the correlation of residual shear strength of the soil with mineralogical composition. *Journal of Geotechnical and Geoenvironmental Engineering*, 131(9), 1139–1150. doi:10.1061/(ASCE)1090-0241(2005)131:9(1139)

Thornburg, T. M., & Kulm, L. D. (1987). Sedimentation in the Chile Trench: Depositional morphologies, lithofacies, and stratigraphy. *Geological Society of America Bulletin*, 98(1), 33–52.

Trütner, S., Hüpers, A., Ikari, M. J., Yamaguchi, A., & Kopf, A. J. (2015). Lithification facilitates frictional instability in argillaceous subduction zone sediments. *Tectonophysics*, 665, 177–185. http://dx.doi.org/10.1016/j.tecto.2015.10.004

Underwood, M. B. (2020). Data report: reconnaissance of bulk sediment composition and clay mineral assemblages: inputs to the Hikurangi subduction system. In L. M. Wallace, D. M. Saffer, P. M. Barnes, I. A. Pecher, K. E. Petronotis, L. J. LeVay, Expedition 372/375 Scientists (Eds.), *Hikurangi subduction margin coring, logging, and observatories, Proceedings of the International Ocean Discovery Program* (Vol. 372B/375). College Station, TX, International Ocean Discovery Program. https://doi.org/10.14379/iodp.proc.372B375.203.2020

Underwood, M. B. (2022). Data report. Clay mineral assemblages within Hikurangi trench-slope deposits, IODP Expedition 372B/375 Site U1519, offshore New Zealand. In L. M. Wallace, D. M. Saffer, P. M. Barnes, I. A. Pecher, K. E. Petronotis, L. J. LeVay, Expedition 372/375 Scientists (Eds.), *Hikurangi subduction margin coring, logging, and observatories, Proceedings of the International Ocean Discovery Program* (Vol. 372B/375). College Station, TX, International Ocean Discovery Program. https://doi.org/10.14379/iodp.proc.372B375.209.2022

Underwood, M. B., & Bachman, S. B. (1982). Sedimentary facies associations within subduction complexes. In J. K. Leggett (Ed.), *Trench-forearc geology, Special Publication* (Vol. 10, pp. 537–550). London, Geological Society.

Underwood, M. B., & Moore, G.F. (1995). Trenches and trench-slope basins. In C. J. Busby, R. V. Ingersoll (Eds.), *Tectonics of Sedimentary Basins* (pp. 179–21). Malden, MA, Blackwell Scientific.

Underwood, M. B., & Dugan, B. (2021). Data report: Clay mineral assemblages within and beneath the Tuaheni landslide complex, IODP Expedition 372A Site U1517, offshore New Zealand. In I. A. Pecher, P. M. Barnes, L.J. LeVay, and Expedition 372A Scientists (Eds.), *Creeping Gas Hydrate Slides*. *Proceedings of the International Ocean Discovery Program* (Vol. 372A). College Station, TX, International Ocean Discovery Program. https://doi.org/10.14379/iodp.proc.372A.201.2021

Underwood, M. B., Lawler, N., & McNamara, K. (2020). Data report: standard mineral mixtures, normalization factors, and determination of error for quantitative X-ray diffraction analyses of bulk powders and clay-sized mineral assemblages. In L. M. Wallace, D. M. Saffer, P. M. Barnes, I. A. Pecher, K. E. Petronotis, L. J. LeVay, Expedition 372/375 Scientists (Eds.), *Hikurangi subduction margin coring, logging, and observatories, Proceedings of the International Ocean Discovery Program* (Vol. 372B/375). College Station, TX, International Ocean

Discovery Program. https://doi.org/10.14379/iodp.proc.372B375.201.2020

Vandorpe, T., Collart, T., Cnudde, V., Lebreiro, S., Hernandez-Molina, F. J., Alonso, B., et al. (2019). Quantitative characterization of contourite deposits using medical CT. *Marine Geology*, 417, 106003. https://doi.org/10.1016/j.margeo.2019.106003

Vanneste, M., Sultan, N., Garziglia, S., Forsberg, C. F., & L'Heureux, J.-S. (2014). Seafloor instabilities and sediment deformation processes: The need for integrated, multi-disciplinary investigations. *Marine Geology*, 152, 183–214. http://dx.doi.org.10.1016/j.margeo.2014.01.005

Warr, L. N., & Cox, S. C. (2016). Correlating illite (Kübler) and chlorite (Árakai) "crystallinity" indices with metamorphic mineral zones of the South Island, New Zealand. *Applied Clay Science*, 134, 164–174. http://dx.doi.org/10.1016/j.clay.2016.06.024.

Watson, S. J., Mountjoy, J. J., & Crutchley, G. J. (2020). Tectonic and geomorphic controls on the distribution of submarine landslides across active and passive margins, eastern New Zealand. In A. Georgiopoulous et al. (Eds.). *Subaqueous mass movements and their consequences: Advances in process understanding, monitoring and hazard assessments*, *Special Publication* (Vol. 500, pp. 477–494). London, Geological Society. https://doi.org/10.1144/SP500-2019-165

Wilson, C. J. N., & Rowland, J. V. (2016). The volcanic, magmatic and tectonic setting of the Taupo Volcanic Zone, New Zealand, reviewed from a geothermal perspective. *Geothermics*, 59, 168–187. http://dx.doi.org/10.1016/j.geothermics.2015.06.013

Yamada, Y., Yamashita, Y., & Yamamoto, Y. (2010). Submarine landslides at subduction margins: Insights from physical models. *Tectonophysics*, 484, 156167. doi:10.1016/j.tecto.2009.09.007